# Supporting Information

**Predicting Supramolecular Self-assembly on Reconstructed Metal Surfaces**

*Thomas J. Roussel*, Esther Barrena, Carmen Ocal, and Jordi Faraudo*

Institut de Ciència de Materials de Barcelona, Consejo Superior de Investigaciones Científicas. (ICMAB-CSIC), Campus de la UAB, Barcelona E-08193, Spain

*Corresponding Author e-mail: troussel@icmab.es

This document contains additional details on the simulations

Before any computational steps, we optimized the molecular atomic structure of the Di-indenoperylene (DIP) molecule. Electrostatic interactions between two neutral DIP molecules arise from an unequal charge distribution over the atoms of each molecule and are described by placing partial charges on the atoms (as shown in **table S1** and **Figure SI.1**). The partial charges were determined according to the Partial Equalization of Orbital Electronegativities (PEOE) algorithm also known as *Gasteiger-Marsili* method.

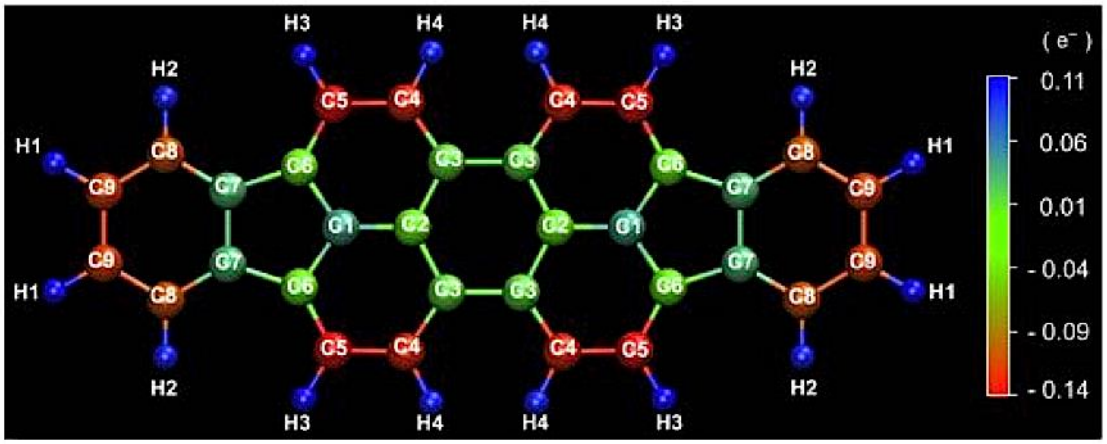


**Figure SI.1 :** Ball & Sticks representation of DIP molecule. Colours are scaled with the partial charges calculated using Material Studio [1, 2].

**Table SI.1:** Partial charges carried by the molecule ($e^{-}$).

| C1 | C2 | C3 | C4 | C5 | C6 | C7 | C8 | C9 | H1 | H2 | H3 | H4 |
|---|---|---|---|---|---|---|---|---|---|---|---|---|
| 0.05 | 0.01 | 0.01 | -0.13 | -0.14 | 0.01 | 0.03 | -0.11 | -0.12 | 0.11 | 0.10 | 0.11 | 0.10 |

We have built an infinite 12 layers slab structure of the Au(111) surface using a semi-empirical many-body potential derived from the tight binding scheme in its second moment approximation (TB-SMA).

After the preliminary steps of molecule-molecule and molecule-surface potential energies precalculation (figure S2 (*left*)), we performed the molecular self-assembly at 300K of 619 DIP molecules (figure S2 (*right*)). Colour scale follows the intermolecular potential energy (kJ $mol^{-1}$). It can be pointed out that rows of molecules are aligned along with the $[1\bar{1}0]$ direction. The molecular azimuthal orientations follow the $[11\bar{2}]$ surface direction.

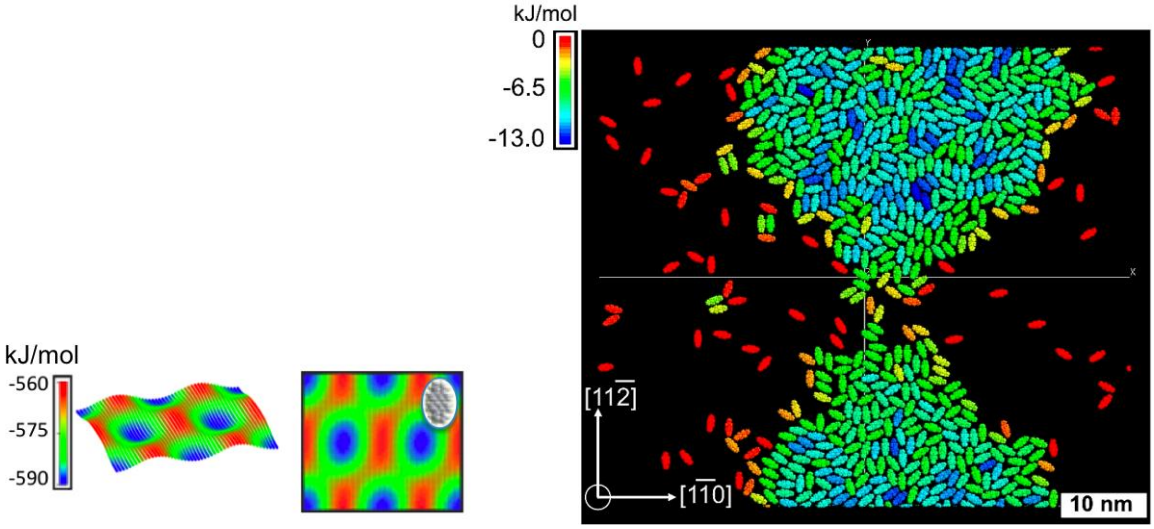


**Figure SI.2 :** (*right*) tilted and top views of the potential energy landscapes of two orthorhombic unit cells of the flat Au(111) surface seen by one DIP molecule oriented along the $[11\bar{2}]$ direction of the substrate. (*left*) Final configuration snapshots with 619 DIP molecules adsorbed on Au(111). Colour scales (in kJ $mol^{-1}$ of molecule) follow the intermolecular potential energy.

Initial configurations for all the MC calculations are prepared with a fixed given number of molecules randomly dispersed on the bare surface. To avoid any early structure formation or

overlap between molecules at the beginning of the simulation, a first MC run of $10^5$ MC attempts per molecule is performed heated at very high temperature (1000K) in order to start the MC computations from a two-dimensional gas phase. Then, the temperature is set at 400K and decreased until we reach 300 K by an increment of 20K between each equilibration. To sample correctly the accessible configuration space, we have performed at least $10^6$ MC attempts per molecule, either by translating, rotating, or a translating and rotating attempt of randomly chosen molecules. At the beginning of the simulation, an initial run of $10^5$ MC (attempts/molecule) is performed with an average displacement equal to half of the simulation box length, which insures a proper and rapid exploration of the accessible configurations (region I of **figure SI.3**). Then, the average displacement is reduced progressively until reaching twice the thermal De Broglie wavelength of the molecule, which is approximately the length of the molecule. Finally, the displacement is calibrated in order to obtain 50% of accepted attempts (region II of fig. SI.3). Once equilibrated, the average values are calculated during the last production run of $10^6$ MC attempts per molecule is performed (region III of fig. SI.3).

The behaviour of the total, intermolecular, and molecule-surface potential energies is represented (figure SI.3) as a function of the number of MC blocks (each block includes $10^5$ attempts of equidistributed translation, rotation, translation and rotation trials). Three equilibration processes are distinguishable during the MC equilibration and addressed in the figure as region (I) where the molecules are allowed to achieve large displacements; (II) the average displacement amplitude is calibrated until reaching 50% acceptance rate of the MC attempts; (III) the production run once the equilibrium is reached. The three configurations in figure 2 of the main manuscript where extracted from each region. Interestingly, despite weak intermolecular interaction, the corresponding potential energy leads the equilibration of the system, while the surface-molecule potential energy varies weakly. Overall, the evolution of energy during the MC simulation shows a decrease of the EMM potential energy and a

modest increase of the molecule-surface EMS. By following the stripes of the substrate (as dictated by molecule-surface interaction), the molecules arrange in configurations that enhance the molecule-molecule interaction and hence promote long-range self-assembly.

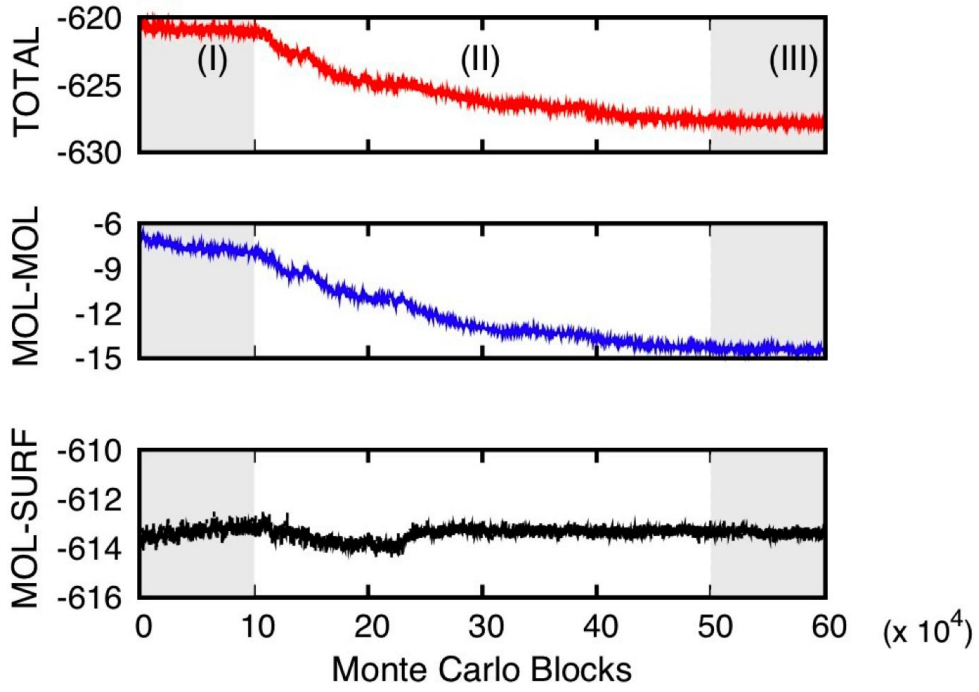


**Figure SI.3 :** Total, intermolecular (MOL-MOL) and molecule-substrate (MOL-SURF) potential energies as a function of the number ($\times 10^4$) of MC blocks (each block includes $10^5$ MC attempts). See in the text for more details.

The Molecular Orientation Distribution (MOD) is represented **Figure SI.4** for the molecular self-assembly of DIP molecules on the Herringbone surface and superposed on the MOD extracted for the infinitely diluted phase adsorbed on the flat Au(111) surface (blue). For clarity, we have tagged the different orientations respectively to the nearest neighbours directions of the substrate (NN), and the next nearest neighbours (NNN) directions, and plotted, below the polar diagram, its linear representation. Note that 0 degree refers to the $[11\bar{2}]$ (NNN green) direction and 90 along the $[1\bar{1}0]$. Black and red MODs correspond to the infinitely diluted and the self-assembled (at 0.41 mol. $nm^{-2}$) phases on the herringbone surface.

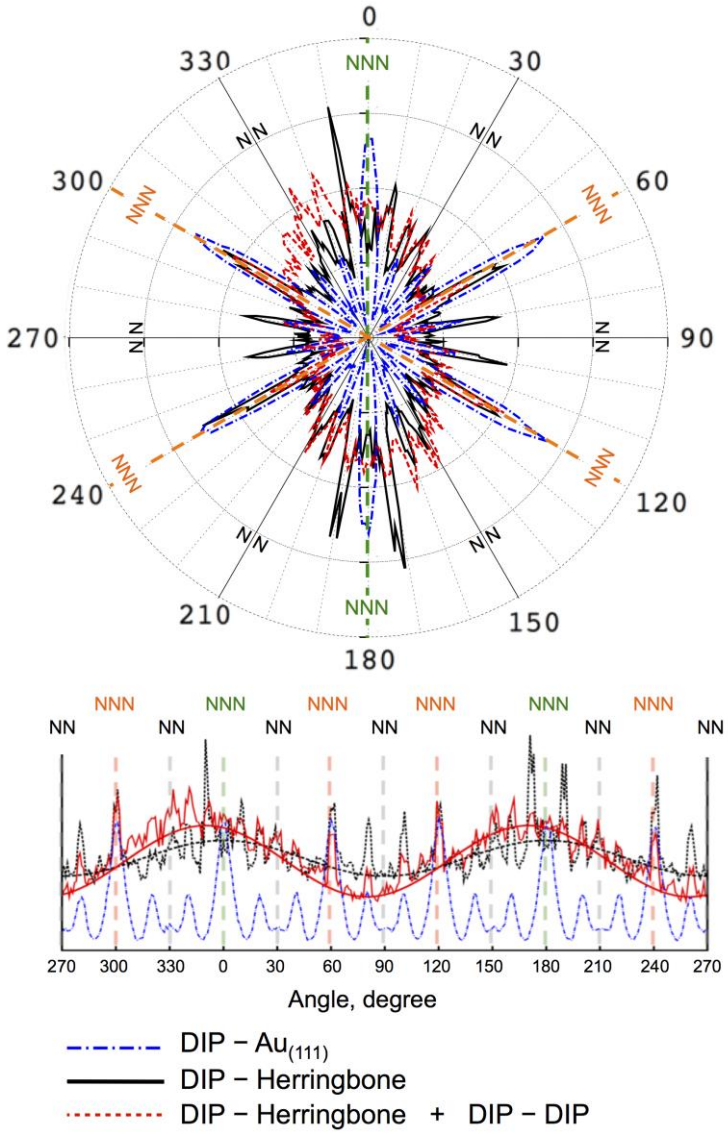


**Figure SI.4 :** Comparative MOD with a flat surface (blue line) of the infinitely diluted phase self-diffusing on the herringbone surface (black line) and during the self-ordering (red line). For clarity, the MOD is also plotted linearly (below the polar diagram).

Three main aspects can be extracted: statistically, 1) the MOD follow preferentially the $[11\bar{2}]$ (NNN green) direction, in other words, the direction of the herringbone pattern; 2) DIP molecules tend to avoid the $[1\bar{1}0]$ direction, but, interestingly, the two other equivalent directions are explored and thus few molecules are perpendicular to the discommensuration lines of the substrate; 3) surprisingly, the molecular orientations split along the $[11\bar{2}]$ direction (at 0 and 180 degrees on the figure) and deviate of 10 degrees which is not the case

along the other NNN directions, therefore along the discommensuration lines directions ([$\bar{2}\bar{1}1$] and [$\bar{1}\bar{2}1$]).

We report below in **Figure SI.5** the molecular self-assembly on the herringbone surface at very low coverage (**SI.5a**), and increasing the coverage (**SI.5b, SI.5c**). The DIP molecules preferentially decorate the pinched and bulged kinks of the reconstruction. As the coverage increases, the occupancy of DIP molecules is notably related to regions with most favourable molecule-substrate interaction and form rows with a tendency to orient the molecular axis with few degrees (about 10°) of deviation from the [$1\bar{1}0$] direction. As the coverage increases further, DIP molecules form compact aggregates without long-range order giving rise to the structure seen in Figure 6 (in the main manuscript) at the highest coverage simulated.

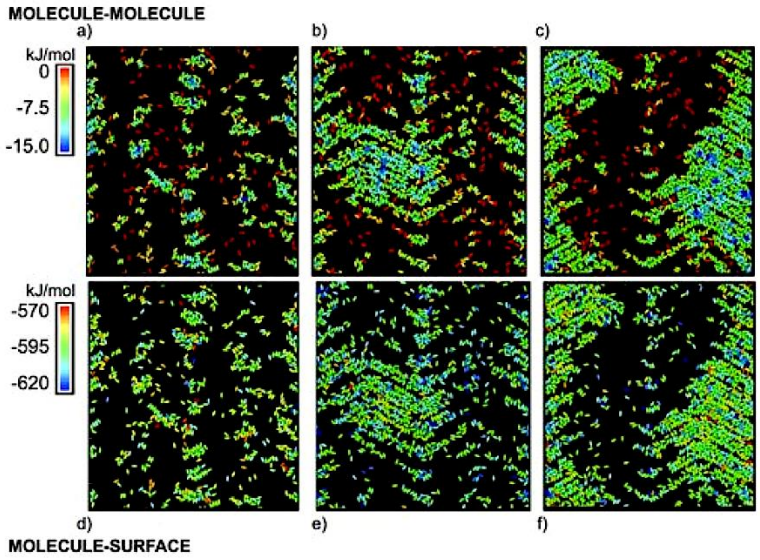


**Figure S.I.5.** Self-assembly of DIP molecules on Herringbone gold surface at different coverage: 600 molecules (a, d), 900 molecules (b, e), and 1200 molecules (c, f).

Below, the structure model proposed by Mendez and Soler (consistently with Barth's previous work) and the STM images of *Roseta* Au(111) stabilized by electrical pulses are shown in **Figure SI.6**.

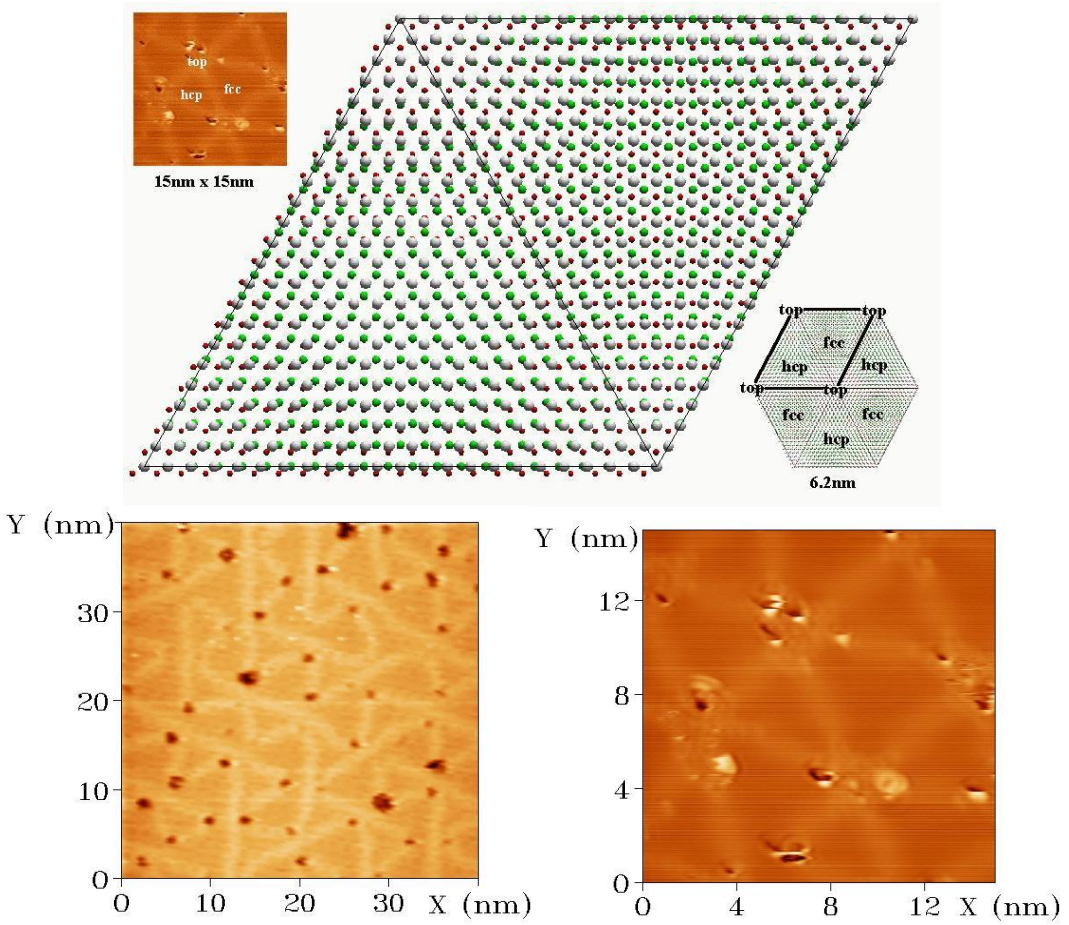


**Figure S.I.6 :** STM images, its atomic structure of the *Roseta* model (provided by Mendez J. and Soler. J.) [3,4]

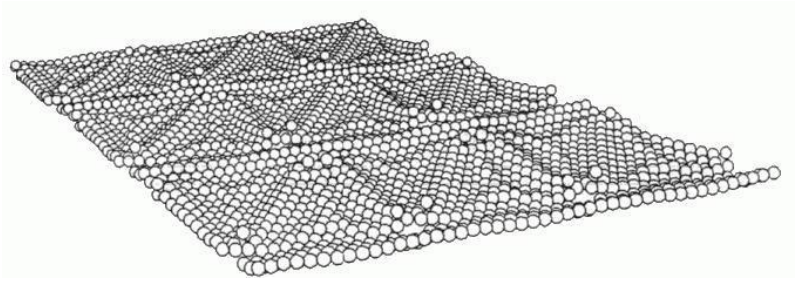

**Figure S.I.7. :** Relaxed atomic structure of the *Roseta* model using a Lennard-Jones potential (provided by Mendez J. and Soler. J.) [3]

Interestingly, Soler J. had attempted to relax this structure model describing with a Lennard-Jones potential (**Figure SI.7**) but this atomic model suffered of the non-realistic description of the metallic bonding which has led to a very distorted surface.

As we previously mentioned in the article on the SANO approach, [5] to relax the surface of the metal, the covalent bonds between the metal atoms are described by a semi-empirical

many-body potential derived from the tight binding scheme proposed by Ducastelle in its second moment approximation (TB-SMA). Gupta has reported that the choose a based-on Friedel's thigh binding model yields physical contraction of face-centred-cubic (100), (110) and (111) surfaces, proper to the square root function of the atomic coordination number. Additionally, they have demonstrated that a simple pairwise potential yields intrinsically to a non-physical expansion of the interlayer distances at the metal surface. This latter unrealistic expansion would prejudice the adsorption potential energy calculation.

We have built a slab structure made of 9 dense layers stacked along z-axis and performed a quenched molecular dynamics (0K) and to provide realistic structural features, the interactions between gold atoms were described by a semi-empirical many-body potential derived from the tight binding scheme in its second moment approximation (TB-SMA). [6,7] We address the structural analyses in the **Figure SI.8** below (left) the density profile of the 9 atomic layers (atom/Å$^3$). Note that the atoms expelled are located at 1.53 Å, which are too few to appear in this density profile. For this reason, we plot (*on the right*) the three top-layers (over the nine) following a colour scale based on the z coordinate (in Å); the bluer the higher.

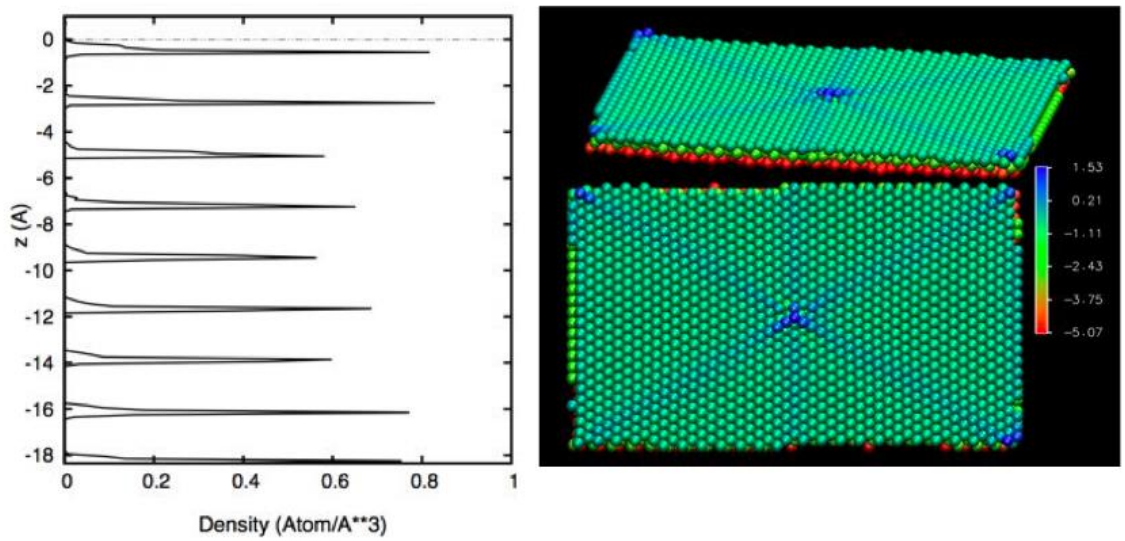


**Figure S.I.8 :** (*right*) Relaxed three first layers of the *Roseta* structure model (Colour scale is based on the z height) and (*left*) its density profile.

**Figure SI.9** below is supporting the figure 4 of the main manuscript. We address the superposition of the polar representation of the molecular orientation distribution for the final configurations (solid red line), the infinitely diluted phase on the flat Au(111) surface (blue dot-dashed line) and the centre of mass (COM) of each molecule for the final configuration of the two homochiral domains reported in figure 4. This plot emphasizes the coexistence of the two domains, the molecular deviation with the $[1\bar{1}0]$ direction, and the alignment of the molecular COM along the $[01\bar{1}]$ and $[\bar{1}01]$ directions (respectively at 30 and at 150 degrees on the polar axis).

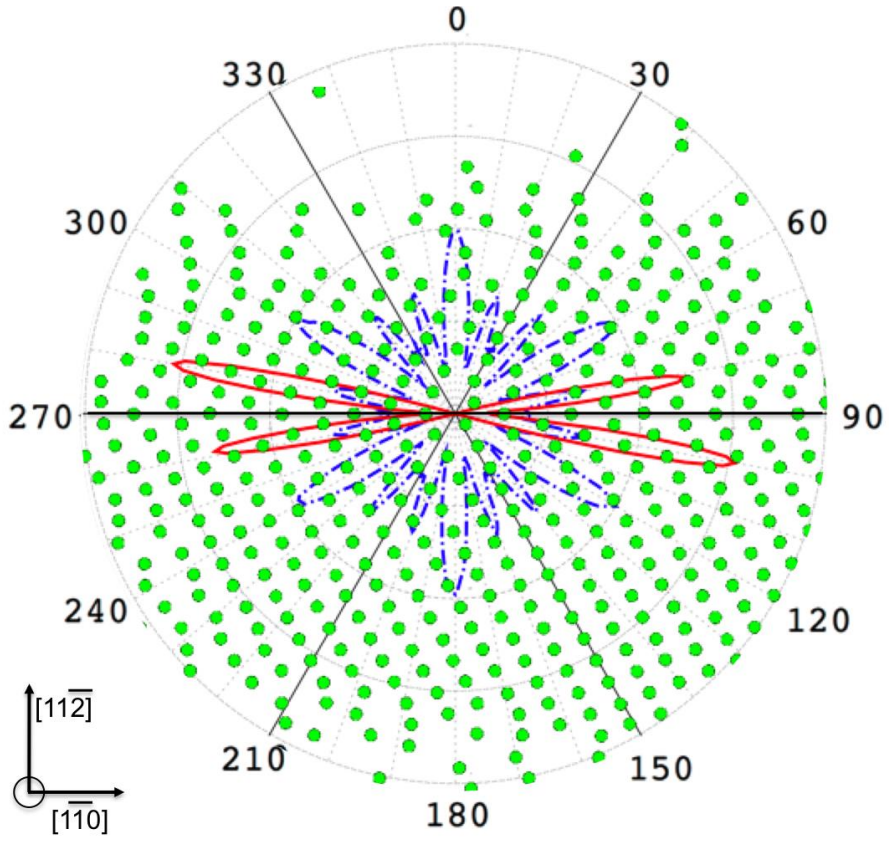


**Figure S.I.9 :** Superposed MOD of the molecular structure (red solid line) extracted from figure 4 in the main manuscript, the infinitely diluted phase adsorbed on the flat (111) surface, and the COM positions of the molecules (green dots).

The results above come from the distorted herringbone model, for which we represent in **Figure SI.10** the potential energy mapping for two molecular orientations.

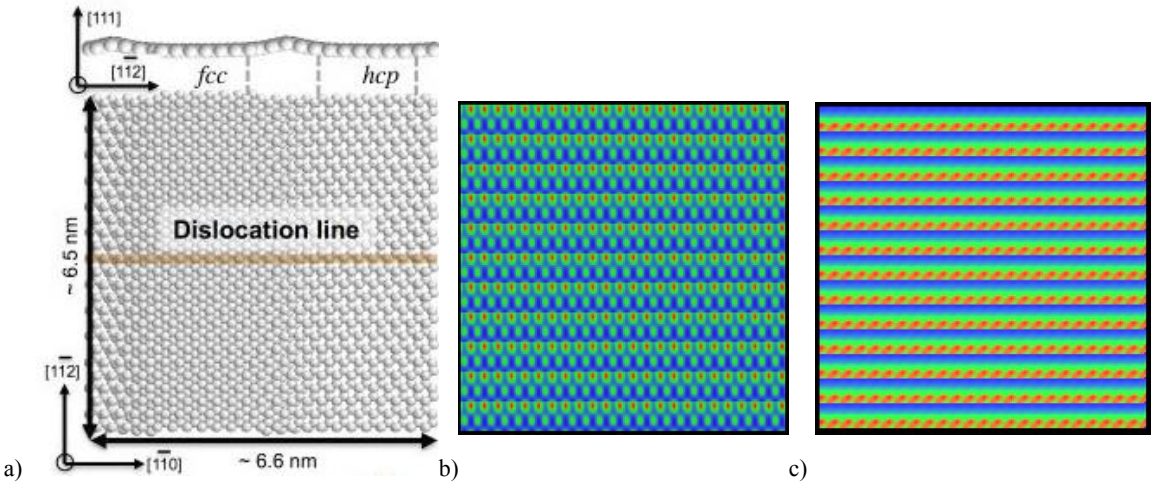


**Figure S.I.10 :** a) the "distorted herringbone" model and the potential energy mappings for two DIP molecular orientation; b) at 0 and c) 90 degrees.

**References for Supporting Information:**

[1] J. Gasteiger, M. Marsili, *Iterative partial equalization of orbital electronegativity—a rapid access to atomic charges*. Tetrahedron, **1980**, *36*, 3219.

[2] Accelrys Software Inc. Materials Studio, Release 5.5. San Diego: Accelrys Software Inc.2010.

[3] J. Mendez, "Modificación y estudio de superficies Au(110) y Au(111) mediante microscopía de efecto túnel en ultra-vacío", *Degree Thesis*, Universidad Autónoma de Madrid, September, **1996**.

[4] J. Mendez, J. Gomez-Herrero, J.I. Pascual, J.J. Saenz, J.M. Soler, A.M. Baro, Diffusion of atoms on Au(111) by the electric field gradient in scanning tunneling microscopy. *J. Vac. Sci. Technol. B*, **1996**, *14*(2), 1145-1148.

[5] T. Roussel, L.F. Vega, Modelling the Self-Assembly of Nano-Objects: Applications to supramolecular organic monolayers adsorbed on metal surfaces. *Journal of Chemical Theory and Computation*, **2013**, *9*, 2161−2169**.**

[6] C. Mottet, G. Tréglia, B. Legrand, Structures of a Ag monolayer deposited on Cu(111), Cu(100), and Cu(110) substrates: An extended tight-binding quenched-molecular-dynamics study. *Phys. Rev. B*, **1992**, 46, 16018.

[7] V. Rosato, M. Guillope, B. Legrand, Thermodynamical and structural properties of f.c.c. transition metals using a simple tight-binding model. *Phil. Mag. A*, **1989**, *59*, 321.